Accepted Manuscript

A chemiluminescence biosensor based on the adsorption recognition function between Fe3O4@SiO2@GO polymers and DNA for ultrasensitive detection of DNA

Yuanling Sun, Jianbo Li, Yanhui Wang, Chaofan Ding, Yanna Lin, Weiyan Sun, Chuannan Luo

PII:	S1386-1425(17)30076-8
DOI:	doi: 10.1016/j.saa.2017.01.057
Reference:	SAA 14910
To appear in:	*Spectrochimica Acta Part A: Molecular and Biomolecular Spectroscopy*
Received date:	1 December 2016
Revised date:	17 January 2017
Accepted date:	25 January 2017

Please cite this article as: Yuanling Sun, Jianbo Li, Yanhui Wang, Chaofan Ding, Yanna Lin, Weiyan Sun, Chuannan Luo , A chemiluminescence biosensor based on the adsorption recognition function between Fe3O4@SiO2@GO polymers and DNA for ultrasensitive detection of DNA. The address for the corresponding author was captured as affiliation for all authors. Please check if appropriate. Saa(2017), doi: 10.1016/j.saa.2017.01.057

A chemiluminescence biosensor based on the adsorption recognition function between Fe_3O_4@SiO_2@GO polymers and DNA for ultrasensitive detection of DNA

Yuanling Sun, Jianbo Li, Yanhui Wang, Chaofan Ding, Yanna Lin, Weiyan Sun, Chuannan Luo*

Key Laboratory of Chemical Sensing & Analysis in Universities of Shandong (University of Jinan), School of Chemistry and Chemical Engineering, University of Jinan, Jinan 250022, China.

Corresponding author: Tel.: +86 0531 89736065. E-mail address: chm_sunyl@126.com

Abstract

In this work, a chemiluminescence (CL) biosensor was prepared for ultrasensitive determination of deoxyribonucleic acid (DNA) based on the adsorption recognition function between core-shell Fe_3O_4@SiO_2 - graphene oxide (Fe_3O_4@SiO_2@GO) polymers and DNA. The Fe_3O_4@SiO_2@GO polymers were composed by GO and magnetite nanoparticles. And the core-shell polymers were confirmed by Scanning Electron Microscope (SEM), X-Ray Powder Diffraction (XRD) and Fourier Transform Infrared (FTIR). Then Fe_3O_4@SiO_2@GO was modified by DNA. Based on the principle of complementary base, Fe_3O_4@SiO_2@GO-DNA was introduced to the CL system and the selectivity, sensitivity of DNA detection was significantly improved. The adsorption properties of Fe_3O_4@SiO_2@GO to DNA were researched through the adsorption equilibrium, adsorption kinetic and thermodynamics. Under optimized CL conditions, DNA could

be assayed with the linear concentration range of 5.0×10^{-12}-2.5×10^{-11} mol/L The detection limit was 1.7×10^{-12} mol/L (3δ) and the relative standard deviation (RSD) was 3.1%. The biosensor was finally used for the determination of DNA in laboratory samples and recoveries ranged from 99% to 103%. The satisfactory results revealed the potential application of Fe_3O_4@SiO_2@GO-DNA-CL biosensor in the diagnosis and the treatment of human genetic diseases.

Keywords: chemiluminescence, DNA determination, Fe_3O_4@SiO_2, graphene oxide, adsorption

1. Introduction

Biological genetic factor - deoxyribonucleic acid (DNA), proposed by Human Genome Project, has got widespread attention by scientific researchers [1]. As the undertaker of genetic information, DNA has been widely used in diagnosis and identification of various diseases [2,3] and the genes detection of genetically modified food [4,5]. In the view of this, various methods including the traditional polymerase chain reaction (PCR) [6-8], hybridization technique [9], capillary electrophoresis (CE) [10,11] , electrochemistry [12-14], fluorescence [15-17] and sensing platforms based on fluorescence [18-19] have been proposed for detection of DNA. However, there are still some respective disadvantages about these methods, such as the low selectivity, timely, poor reproducibility and poor repeatability. Thus, seeking for a simple, effective, selective and sensitive method to detect DNA becomes significantly important.

Chemiluminescence (CL) is a detection method based on the quantitative relationship between the emission intensity (*I*) that liberates energy by emitting light

and the concentration (*c*) of measured molecular which is usually a catalyst, an inhibitor, a reaction product, or an additive in a chemical reaction process [20,21]. The CL technology is of high sensitivity, low background interference and simple instrumentation, and has developed to be a widely applied technology in analysis field [22,23]. However, its extensive application was restricted by low selectivity which could be improved by using some materials with specific recognition capability in the CL system [24].

Graphene oxide (GO) is a kind of two-dimensional carbon materials with large specific surface area and good adsorption capacity. The surface of GO contains a lot of epoxy, hydroxy and carboxy groups, which make it easily to form GO polymers with other materials [25,26]. As a kind of GO polymers, magnetic graphene oxide (MGO) has large specific surface area and can be easily separated with matrix. It has been widely used in many significant fields [27], especially in biological applications. Jiang prepared hydrophilic MGO polymers (GO/Fe_3O_4/Au/PEG) and used it successfully in highly selective enrichment of glycopeptides [28]. Surface molecularly imprinted polymer-ionic liquid modified Fe_3O_4@dopamine/graphene oxide/β-cyclodextrin (ILs-Fe_3O_4@DA/GO/β-CD-SMIPs) was been prepared and an ultrasensitive lysozyme chemiluminescence biosensor was composed [29]. Compared with other biocompatible materials, SiO_2 composite materials has played an important role in biomedical field because of not only its good biocompatibility, low toxicity to biological cells and tissues, but its excellent characteristics of simple preparation, stable nature and easy to modify the surface [30]. Fe_3O_4@SiO_2, a core-shell cladding

material, combines good biocompatibility performance of SiO_2 and easy separation characteristics of Fe_3O_4. It has widely used in the field of biological sensing and analysis [31,32]. Fe_3O_4@SiO_2@GO has been synthesized by other scientists and applied to detect some analytes [33-37], but most only involved the study of adsorption properties [33,36] and detected analytes by extraction [34], liquid chromatography [35]，fluorescence [35,37]. Those methods also have complex operations and poor specificity. At present, it has not been reported to introduce Fe_3O_4@SiO_2@GO to the CL based on the principle of complementary base pair and realize the selective, sensitive and simple detection of DNA.

In this study, the polymers - Fe_3O_4@SiO_2@GO were synthesized based on the good biocompatibility performance of SiO_2, easy separation characteristics of Fe_3O_4 and the large adsorption surface area of GO. Then, the Fe_3O_4@SiO_2@GO polymers were used to form an ultrasensitive chemiluminescence DNA biosensor for the determination of DNA based on the adsorption recognition function between Fe_3O_4@SiO_2@GO and DNA. Finally, the biosensor was used for the detection of DNA in laboratory samples.

2. Experimental

2.1 Materials

DNA sequences (the sequence of A：5'-GAGGTCATGGTGGCGGCAGCGCCT CACAACCTC-3'，the coordination sequence of B and other sequences (DNA1, DNA2, DNA3, DNA4)) were purchased from Sangon Biotech Company (Shanghai, China). Graphite Powder was purchased from Tianjin Hongyan Chemical Reagent

Factory (Tianjin, China). Tetraethoxysilane (TEOS 28%, the calculation of SiO_2, AR) was supplied by Tianjin Chemical Reagent Factory (Tianjin, China). Fe_3O_4 nanoparticles and N-(3-Aminopropyltriethoxysilane) (APTES, AR) were supplied by Shanghai Crystal Biochemical Technologies Inc (Shanghai, China). 1-Ethyl-3-(3-dimethylaminopropyl) carbodiimide hydrochloride (EDC, AR) and H-Hydroxysuccinimide (NHS， AR) were purchased from Shanghai Chemical Technology Co., Ltd. (Shanghai, China). Luminal, ethanol, sodium hydroxide, potassium permanganate and all other chemicals unless specified were analytical reagent grade and used without further purification.

Redistilled water was used throughout the work. Phosphate buffer (PBS, pH=7.4, 0.01 mol/L) solution was used to prepare all DNA solutions, which was stored in a refrigerator (4 ˚C).

2.2 Apparatus

The IFFM-E flow injection CL analyzer (Xi'an Remex Electronic instrument High-Tech Ltd, China) was equipped with an automatic injection system and a detection system. The morphology of the SiO_2@Fe_3O_4@GO nanoparticles were characterized using a SEM (GUANTA FEG 250, FEI, America). The XRD measurements were made on a D8 focus spectrometer (Brooke AXS, Germany). The FTIR was used in characterization of functional groups (PerkinElmer Corporation, American).

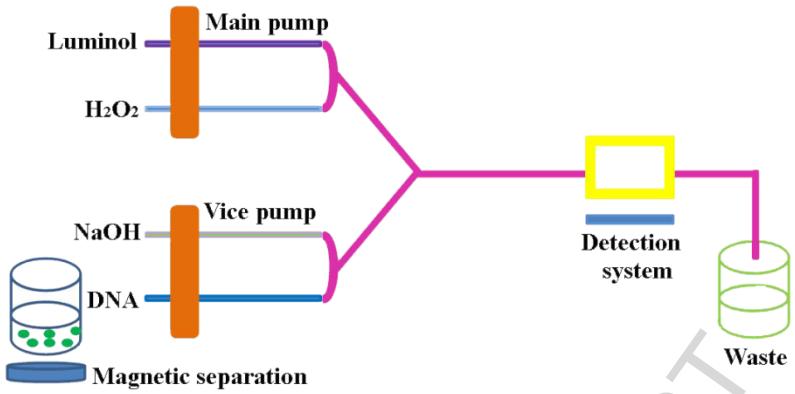

Fig.1. Operating principle diagram of the IFFM-E system.

2.3 Preparation of GO

GO was prepared by a modified Hummers method procedure described in previous literatures from our group and other people, respectively [38]. Briefly, 180 mL of H_2SO_4 was added into a 500 mL three mouth flask followed by adding 1.0 g of graphite powders. Then, 6.0 g of potassium permanganate was added and the whole system was stirred for 2 h. And the diluted suspension was stirred for 12 h at 90 ˚C. Finally, 30% H_2O_2 was dropped until no bubbles were formed. After the reaction, the mixture was filtered, and washed by 0.2 mol/L HCl and ultrapure water, respectively, till the pH=7.0. The obtained product was dried for use.

2.4 Preparation of Fe_3O_4@SiO_2

Fe_3O_4@SiO_2 was prepared by a modified Stober hydrolysis method [39]. 0.3 g of Fe_3O_4 nanoparticles were added into a 150 mL round bottom flask in which ethanol/water (w_1/w_2=1:1) solution was already added and stirred for 15 min. Then 5 mL of ammonia and 2 mL of APTES were dropped in the flask and reacted for 12 h at 50 ˚C. Finally, Fe_3O_4@SiO_2 was collected by magnetic separation, washed with water, and dried under vacuum.

2.5 Preparation of Fe_3O_4@SiO_2@GO

0.5 g of Fe_3O_4@SiO_2 was added to 5 mL of APTS and 20 mL of anhydrous toluene solution, and reacted for 12 h under the atmosphere of N_2 at 50 ˚C. Then the product was collected by magnetic separation and washed with water till pH=7.0. Finally, the obtained composites - Fe_3O_4@SiO_2-NH_2 was dried under vacuum.

0.2 g of GO was dispersed in 100 mL of water. Afterwards, 3 mg of EDC and 28 mg of NHS were added into the solution. Then, 200 mg of Fe_3O_4@SiO_2-NH_2 was added to the solution, and stirred for 30 min. Subsequently, the mixture reacted for 2 h at 80 ˚C. The final product was separated, washed, and dried.

2.6 Adsorption properties of Fe_3O_4@SiO_2@GO

Adsorption isotherm: 5.0 mg of Fe_3O_4@SiO_2@GO was placed into 10 mL colorimetric tubes. Then, different volume doses of 2.0×10^{-11} mol/L of DNA solution were added to the tubes, respectively, and the tubes were shaken at 25˚C for 1 h. After magnetic separation, the concentration of the supernatant in the tubes was determined by a CL instrument and the adsorption capacities were calculated.

Rebinding dynamics: 5.0 mg of Fe_3O_4@SiO_2@GO was dispersed in 12.0 mL of 2.0×10^{-11} mol/L of DNA solution which then were shaken for 1 min, 3 min, 5 min, 10 min, 15 min, 30 min, 45 min and 60 min, respectively. After magnetic separation, the concentration of the supernatant in the tube was determined by a CL instrument and the adsorption capacities were calculated.

The adsorption capacity was calculated from the following formula:

$$Q_e = (c_0 - c_e)V/m$$

Where Q_e (mol/mg) was the mass of DNA adsorbed per unit mass of dry particles, c_0 (mol/L) and c_e (mol/L) were the concentrations of the initial and balance solution, respectively, V (L) was the total volume of the adsorption mixture, and m (mg) was the mass of Fe_3O_4@SiO_2@GO added.

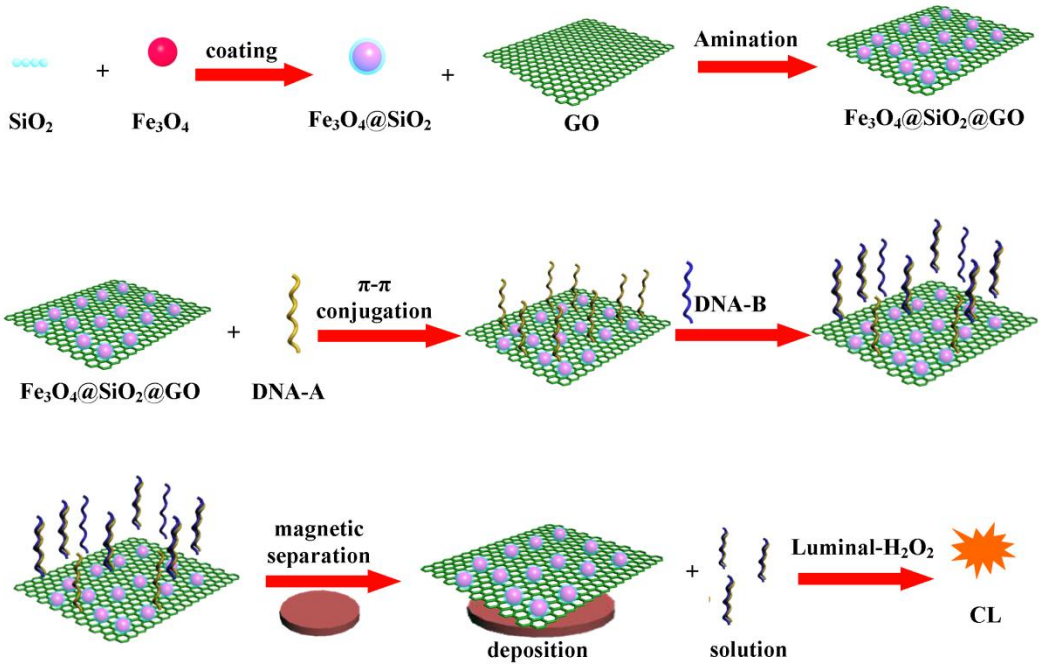

Fig. 2. The preparing process of Fe_3O_4@SiO_2@GO and the schematic diagram of biosensor.

3. Results and discussion

3.1 Characterization of GO, Fe_3O_4@SiO_2 and Fe_3O_4@SiO_2@GO

Fig. 3(A) shows the FTIR of GO, Fe_3O_4@SiO_2 and Fe_3O_4@SiO_2@GO. The peaks at 1400-1600 cm^{-1} are characteristic peaks of the benzene ring. In the spectrum of GO, the absorption band with strong intensity and shape at 1703 cm^{-1} is the stretching vibration of the C=O band. In the spectrum of Fe_3O_4@SiO_2, the peak at 586 cm^{-1} is the characteristic peak of Fe_3O_4 nanoparticles, and the peaks at 805 cm^{-1}, 463 cm^{-1} attribute to the stretching vibration of the Si-O-Si band and O-Si-O band,

respectively. In the spectrum of Fe_3O_4@SiO_2@GO, the peak at 1126 cm^{-1} is the stretching vibration of C-N. When reacted with -NH_2, the peak of C=O at 1703 cm^{-1} shifted to 1780 cm^{-1}, which confirmed the reaction of Go and aminated Fe_3O_4@SiO_2. Fig. 3(B) illustrates the XRD patterns of the obtained GO, Fe_3O_4@SiO_2 and Fe_3O_4@SiO_2@GO. Obviously, the characteristic peak of GO situated at 2θ=10.6°. It also displays several diffraction rings at 2θ=30.2°, 35.6°, 43.4°, 53.3°, 57.5° and 63.1°, which corresponded to (2 2 0), (3 1 1), (4 0 0), (4 2 2), (5 1 1), and (4 4 0), the six indices of the Fe_3O_4 inverse spinel structure. And the characteristic peak of SiO_2 situated at 2θ=26.0°. The satisfying results further provided remarkable support that Fe_3O_4@SiO_2@GO polymers were successfully prepared.

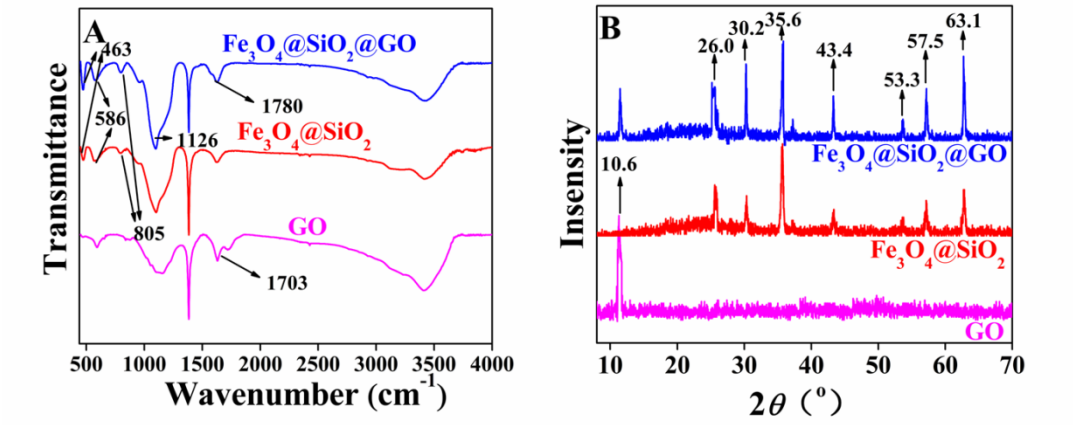

Fig. 3. The FTIR of GO, Fe_3O_4@SiO_2 and Fe_3O_4@SiO_2@GO (A), and XRD patterns of obtained GO, Fe_3O_4@SiO_2 and Fe_3O_4@SiO_2@GO (B).

In Fig. 4, SEM was used to characterize the surface morphology of the GO, Fe_3O_4@SiO_2 and Fe_3O_4@SiO_2@GO. As shown in Fig. 4(A), a wrinkled and thin film was observed in the image of GO, which demonstrated the large specific surface area of GO. Fig. 4(B) clearly reveals that Fe_3O_4 nanoparticles were presented as a relative regular spherical structure, and SiO_2 was successfully coated on the Fe_3O_4 surface. As

shown in Fig. 4(C), GO sheets were displayed clearly by a loose 3D network structure consisting of 2D. And Fe_3O_4@SiO_2 nanoparticles were immobilized onto the GO films, which increases the surface area and serves as a supporting interface to combine with other functional groups.

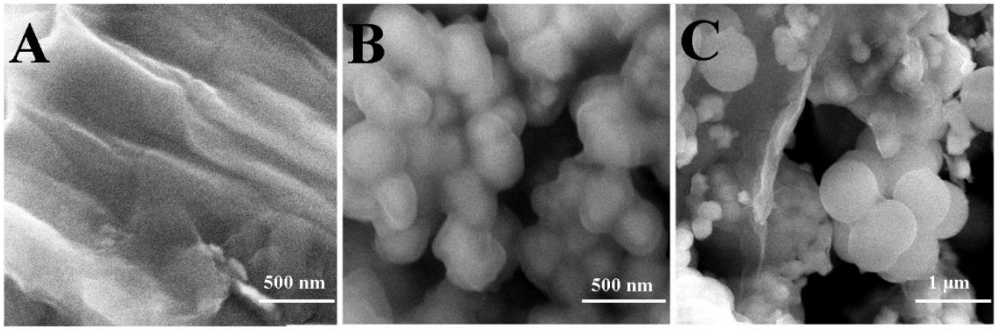

Fig. 4. The surface morphology of GO (A), Fe_3O_4@SiO_2 (B) and Fe_3O_4@SiO_2@GO (C) in SEM images.

3.2 Adsorption properties of Fe_3O_4@SiO_2@GO

The adsorption performance of Fe_3O_4@SiO_2@GO for DNA was measured and shown in Fig. 5. The adsorption capacities for DNA at different initial concentrations, i.e. the adsorption isotherms, are shown in Fig. 5(A).The adsorption capacity for DNA increased with increasing DNA concentration before reaching a maximum of 3.24 $\times 10^{-9}$ mol/mg, which was higher than the adsorption capacity of Fe_3O_4@SiO_2（1.78 $\times 10^{-9}$ mol/mg）at the same conditions. Fig. 5(B) showed the adsorption kinetics of Fe_3O_4@SiO_2@GO for DNA. Fe_3O_4@SiO_2@GO particles could reach maximum adsorption easily with in 15 min compared to Fe_3O_4@SiO_2 particles (30 min), and that can be contribute to the strong conjugation and fast mass transfer between GO and DNA.

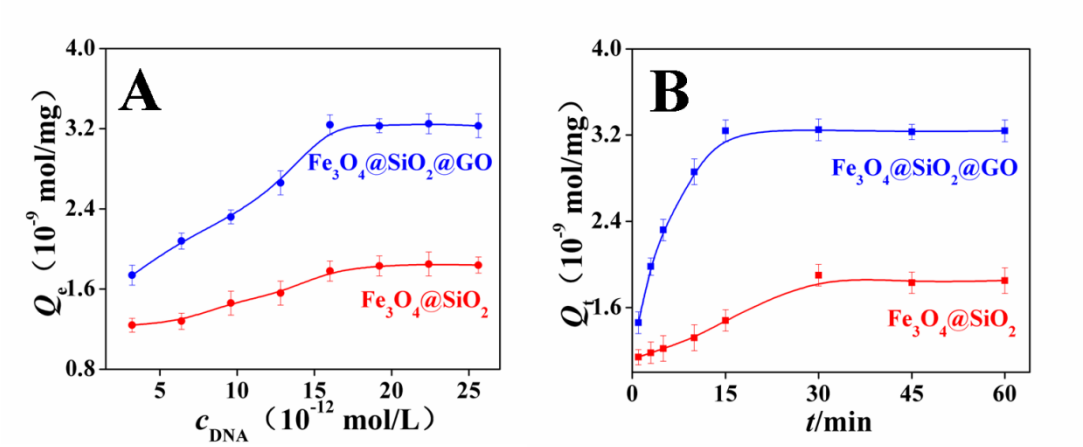

Fig. 5. Adsorption isotherm curves (A) and adsorption kinetics curves (B) of $Fe_3O_4@SiO_2@GO$.

3.2.1 Adsorption isotherm of $Fe_3O_4@SiO_2@GO$

The Langmuir and Freundlich equations [40,41] were respectively used for modeling adsorption isotherms. As shown in Fig. 6(A,B), the linear fitting curves of the Langmuir (R^2=0.9754) and Freundlich (R^2=0.9410) models indicated that the Langmuir isotherm was more appropriate than the Freundlich model for the relative standard deviation values. The results revealed that the proposed adsorption process on the surface of $Fe_3O_4@SiO_2@GO$ was mainly monolayer uniform adsorption [40,41]. Therefore, it indicated that $Fe_3O_4@SiO_2@GO$ enabled easy access to DNA.

3.2.2 Adsorption kinetics of $Fe_3O_4@SiO_2@GO$

In order to provide more complete insight into the adsorption processes, two adsorption kinetic equations [42,43] shown in Fig. 6(C,D) (pseudo-first order (C) and pseudo-second order (D)) were applied to model the kinetics of DNA adsorption on $Fe_3O_4@SiO_2@GO$ particles. Better correlation was observed in the pseudo-second order model (R^2=0.9874). It was confirmed that $Fe_3O_4@SiO_2@GO$ followed pseudo-second order sorption kinetics [42,43] when binding DNA. The theoretical

adsorption capacity (Q_{tm}) of Fe_3O_4@SiO_2/GO to DNA was obtained at 3.33×10^{-9} mol/mg, which was similar to the experimental result, 3.24×10^{-9} mol/mg.

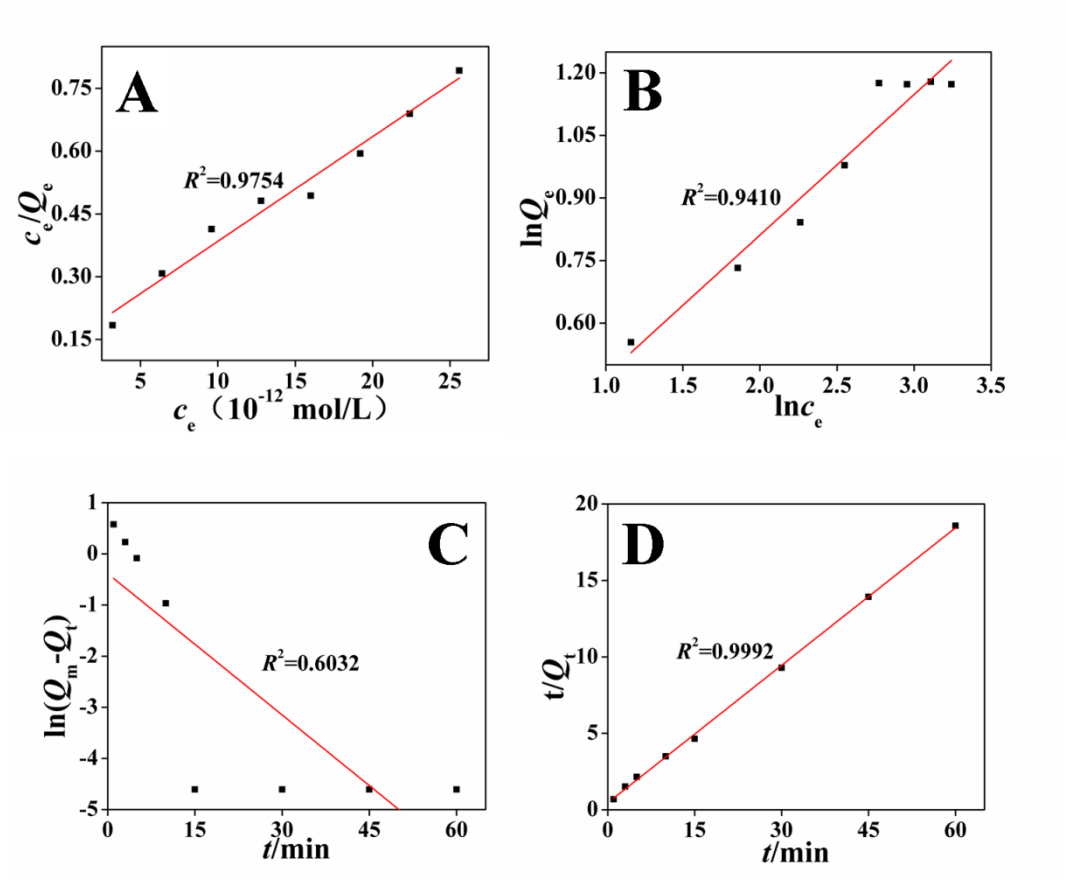

Fig. 6. Adsorption isotherm equation of Fe_3O_4@SiO_2@GO for DNA: Langmuir model (A) and Freundlich model (B); Adsorption kinetics of Fe_3O_4@SiO_2@GO for DNA: pseudo-first order (C) and pseudo-second order (D).

3.3 Optimization of the Fe_3O_4@SiO_2@GO-DNA-CL biosensor

The adsorption time which depended on peristaltic pumps speed was an important parameter for the adsorption capacities of DNA on the surface of Fe_3O_4@SiO_2@GO. When pumps speed was too high, DNA molecules could not be absorbed by Fe_3O_4@SiO_2@GO completely. And when pumps speed was too low, the other substances in the samples would be absorbed by Fe_3O_4@SiO_2@GO. Thus, 30 rpm for main pump speed and 35 rpm for vice pump speed were optimized between

20 and 45 rpm for further work.

The concentrations of NaOH, luminol and H_2O_2 would affect the CL intensity, and were chosen as showed in Fig. 7(A-C). In which, ΔI was the CL signal difference between the solution containing DNA and the blank solution. As could be seen that the maximum CL intensity could be obtained at the concentration of NaOH: 0.2 mol/L, luminol: 5.0×10^{-5} mol/L, and H_2O_2: 0.25 mol/L simultaneously.

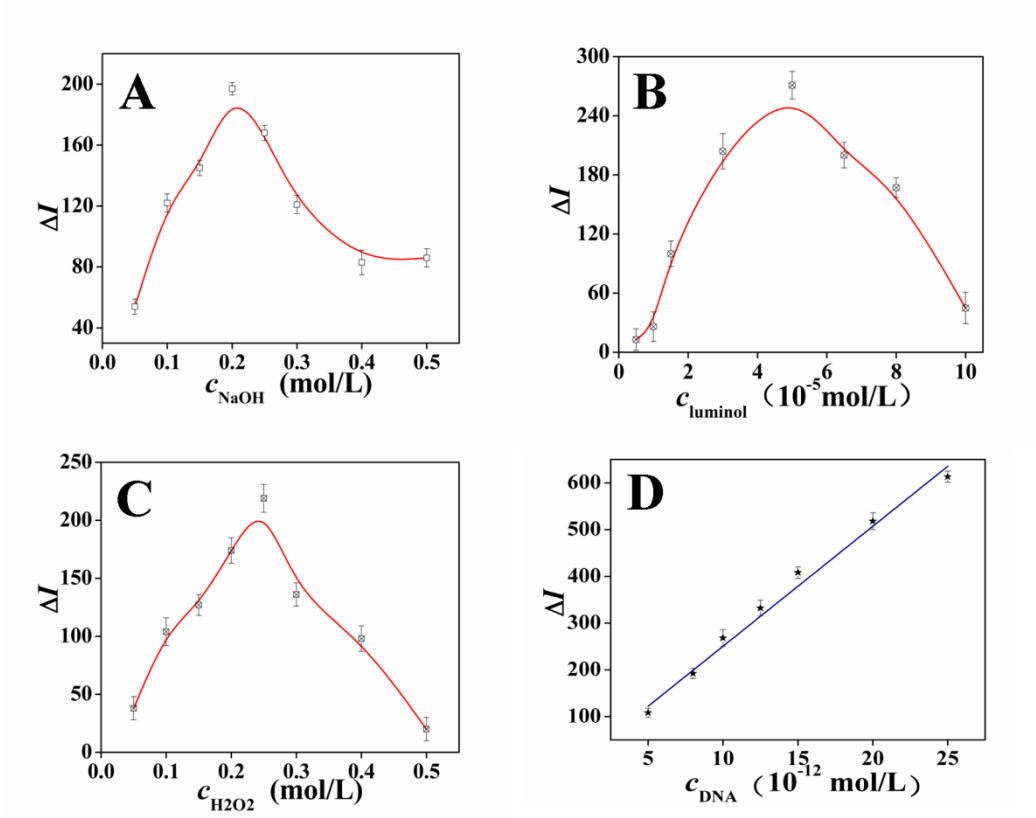

Fig. 7. Optimization results: effect of NaOH (A), luminol (B), H_2O_2 (C) concentration on CL intensity; Regression equation of the Fe_3O_4@SiO_2@GO-DNA-CL biosensor (D).

3.4 Analytical performance of theFe_3O_4@SiO_2@GO-DNA-CL biosensor

Under the optimal conditions, the analytical performance of the described Fe_3O_4@SiO_2@GO-DNA-CL biosensor was studied. The regression equation shown in Fig. 6(D) was described by the calibration curve ΔI=-6.33+2.57×$10^{12}c$ (c: mol/L,

R^2=0.9875), and the detection range of DNA was from 5.0×10^{-12} to 2.5×10^{-11} mol/L. The detection limit was 1.7×10^{-12} mol/L (3δ) with a relative standard deviation (RSD) of 3.1% (*n*=11). The results were compared with those of traditional methods as shown in Table 1. The Fe_3O_4@SiO_2@GO-DNA-CL biosensor exhibited a relatively low detection limit and high sensitivity to DNA.

Table 1. Comparing results with conventional methods.

Method	Linear range (mol/L)	Detection limit (mol/L)
Our work	5.0×10^{-12} to 2.5×10^{-11}	1.7×10^{-12}
PCR [8]	1.0×10^{-11} to 1.0×10^{-8}	4.0×10^{-12}
Hybridization technique [9]	0 to 7.0×10^{-9}	5.0×10^{-11}
CE[11]		5.0×10^{-12}
Electrochemistry [14]	1.0×10^{-9} to 1.0×10^{-4}	
Fluorescence[17]	1.0×10^{-11} to 1.0×10^{-10}	1.0×10^{-12}
Sensing fluorescence[19]	5.0×10^{-11} to 1.0×10^{-9}	5.0×10^{-11}

3.5 Selectivity studies of the Fe_3O_4@SiO_2@GO-DNA-CL biosensor

To evaluate the selectivity of the biosensor for DNA, different analytes with increasing amounts were added in standard DNA solution involving lysozyme, L-tryptophan, DNA 1(the sequence：5'-GTGGGTAGGGCGGGTTGG-3') and DNA2 (the sequence：5'-GGAAGGTGTGGAAGG-3'), respectively and it was shown in Fig. 8(A). In the Fe_3O_4@SiO_2@GO-DNA-CL biosensor, 700 and 550 times of lysozyme, L-tryptophan respectively would interfere the determination of DNA. Compared to the conventional CL biosensor (130 and 95 times respectively), the Fe_3O_4@SiO_2@GO-DNA-CL biosensor had stronger ability to resist interferences and was more adequate for the detection of DNA. The selectivity of CL was also

significantly improved by the introduction of Fe_3O_4@SiO_2@GO-DNA. Whereas the interference from DNA1 and DNA2 was relatively serious, this may because they had similar structural units between DNA and DNA1 (or DNA2). Fig.8(B) showed the selectivity performances of the Fe_3O_4@SiO_2@GO-DNA-CL biosensor to five different nucleotides - DNA, DNA1, DNA2, DNA3 (the sequence：5'-AGTCCGTGGTAGGGCAGGTTGGGGTGACT-3') and DNA4 (the sequence：5'-TGGGGGTTGAGGCTAAGCCGAAGCCGA-3') in PBS solutions. Compared DNA with other nucleotides, the Fe_3O_4@SiO_2@GO-DNA exhibited much higher binding amounts for DNA. Interferences were eliminated or reduced by the application of Fe_3O_4@SiO_2@GO and the complementary base pairing reactions of DNA in the CL biosensor.

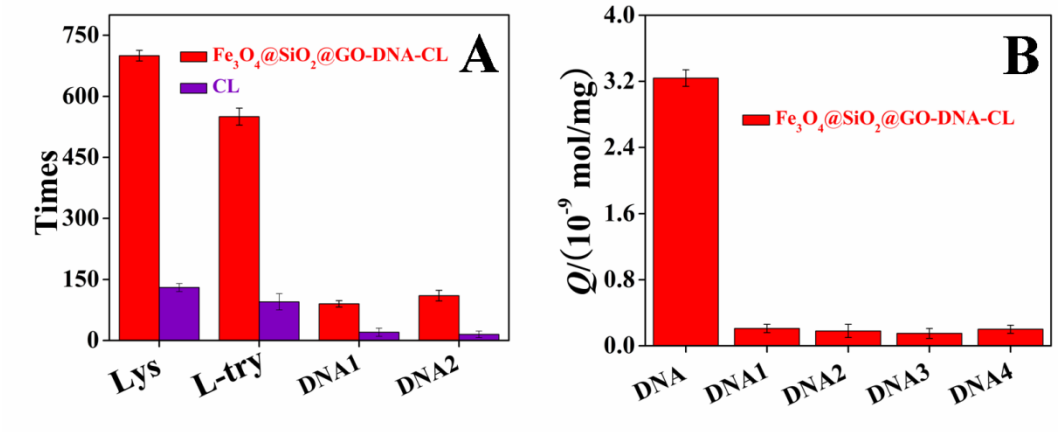

Fig. 8. Interferences study of the Fe_3O_4@SiO_2@GO-DNA-CL biosensor (A); Binding amounts of different nucleotideson the Fe_3O_4@SiO_2@GO-ssDNA (B).

3.6 Recyclability of the Fe_3O_4@SiO_2@GO-DNA-CL biosensor

The recyclability of Fe_3O_4@SiO_2@GO, an important parameter of the biosensor, was evaluated by reusing Fe_3O_4@SiO_2@GO. Because the force of complementary pairing of base pairs is larger than the conjugate effect between Fe_3O_4@SiO_2@GO

and DNA, DNA was removed from the surface of Fe_3O_4@SiO_2@GO when the complementary DNA strand was present. The adsorption capacity of used Fe_3O_4@SiO_2@GO was obtained and then compared with the adsorption capacity of Fe_3O_4@SiO_2@GO before any use. The result showed that there was 3% adsorption capacity loss in 4 times. So it manifested that Fe_3O_4@SiO_2@GO was very suitable in the quantification detection of DNA.

3.7 Application of theFe_3O_4@SiO_2@GO-DNA-CL biosensor

As is shown in Table 2, under the optimal experimental conditions, the Fe_3O_4@SiO_2@GO-DNA-CL biosensor was applied in biological samples which were made by the mixing solution containing an unknown amount of DNA and other interfering substance. Obviously, the recoveries varied from 91% to 103%. These results showed that the biosensor had good accuracy in the determination of DNA. Therefore, the Fe_3O_4@SiO_2@GO-DNA-CL biosensor has provided the possibility of measuring the content of DNA in biological samples.

Table 2. Application of the Fe_3O_4@SiO_2@GO-DNA-CL biosensor.

Sample	c (10^{-12} mol/L)	c_{added} (10^{-12} mol/L)	c_{found} (10^{-12} mol/L)(n=6)	RSD (%)	Recovery (%)
1	11.9	20.0	31.9	3.4	100
2	10.3	20.0	30.9	3.2	103
3	9.6	20.0	27.8	2.6	91

4 Conclusions

Based on the application of multifunctional material and the complementary base pairing reactions of DNA, the novel CL biosensor was proposed based on the adsorption recognition function between Fe_3O_4@SiO_2@GO polymers and DNA. The

Fe_3O_4@SiO_2@GO biosensor showed relatively high capacity to DNA owing to the conjugation effect between the polymers and DNA. The maximum adsorption capacity of Fe_3O_4@SiO_2@GO reached 3.24×10^{-9} mol/mg and the binding process followed the Langmuir isotherm equation and pseudo second order sorption kinetics. The sensitivity and selectivity of biosensor was significantly improved by the application of CL technique based on the reactions of complementary base pair between Fe_3O_4@SiO_2@GO-DNA and complementary nucleotide chains. Simultaneously, the accuracy, reusability and mechanical stability were improved when the polymers were used to determine DNA in laboratory samples. The satisfactory results revealed the potential application of Fe_3O_4@SiO_2@GO-DNA-CL biosensor in the diagnosis and the treatment of human genetic diseases.

Acknowledgements

This work was supported by the Shandong Provincial Natural Science Foundation of China (No. ZR2012BM020) and the Scientific and technological development Plan Item of Jinan City in China (No. 201202088).

References

[1] Y.M. Thu, A.K. Bielinsky. Enigmatic roles of Mcm10 in DNA replication. Trends in Biochemical Sciences, 2013, 38(4): 184-194.

[2] K. Lam, K. Pan, J.F. Linnekamp, J.P. Medema, R. Kandimalla. DNA methylation based biomarkers in colorectal cancer: A systematic review. Biochimicaet Biophysica Acta – Reviews, 2016, 1866(1): 106-120.

[3] M.K. Amir, S.Z. Khan, F. Hayat, A. Hassan, I.S. Butler, Z. Rehman. Anticancer activity, DNA-binding and DNA-denaturing aptitude of palladium(II) dithiocarbamates. Inorganica Chimica Acta, 2016, 451: 31-40.

[4] X. Mi, J. Yang, L. Cao, X. Wei, Y. Zhu, Q.Y. Li, et al. Potential DNA markers as a rapid tracing tool for animal adulterants invegetarian food. Food Research International, 2015, 76: 926-931.

[5] M. Tagliavia, A. Nicosia, M. Salamone, G. Biondo, C.D. Bennici, S. Mazzola, et al. Development of a fast DNA extraction method for sea food and marine species identification. Food Chemistry, 2016, 203: 375-378.

[6] S.K. Jha, R. Chand, D. Han, Y.C. Jang, G.S. Ra, J.S. Kim, et al. An integrated PCR microfluidic chip incorporating aseptic electrochemical cell lysis and capillary electrophoresis amperometric DNA detection for rapid and quantitative genetic analysis. Lab on A Chip, 2012, 12(21): 4455-4464.

[7] I.P.M. Lau, E.K.S. Ngan, J.F.C. Loo, Y.K. Suen, H.P. Ho, S.K. Kong. Aptamer-based bio-barcode assay for the detection of cytochrome-c released from apoptotic cells. Biochemical and Biophysical Research Communications,

2010, 395(4): 560-564.

[8] Z. Li, W. Zhu, J Zhang, J. Jiang, G. Shen, R. Yu. A label-free amplified fluorescence DNA detection based on isothermal circular strand-displacement polymerization reaction and graphene oxide. Analyst, 2013, 138(13): 3616-3620.

[9] N. Li, X. Hao, B.H. Kang, Z Xu, N.B. Li, H.Q. Luo, et al. Enzyme-free fluorescent biosensor for the detection of DNA based on core–shell Fe_3O_4 polydopamine nanoparticles and hybridization chain reaction amplification. Biosensors and Bioelectronics, 2015, 77: 525-529.

[10] C. Li, H. Wang. Selective enzymatic cleavage and labeling for sensitive capillary electrophoresis laser-induced fluorescence analysis of oxidized DNA bases. Journal of Chromatography A, 2015, 1406:324-330.

[11] M. He, K. Li, J. Xiao, Y. Zhou. Rapid bio-barcode assay for multiplex DNA detection based on capillary DNA Analyzer. Journal of Virological Methods, 2008, 151(1): 126-131.

[12] X. Zhang, H. Su, S. Bi, S. Li, S. Zhang. DNA-based amplified electrical bio-barcode assay for one-pot detection of two target DNAs. Biosensors and Bioelectronics, 2009, 24(8): 2730-2734.

[13] B.J. Marsh, L. Hampton, S. Goggins, C.G. Frost. Fine-tuning of ferrocene redox potentials towards multiplex DNA detection. New Journal of Chemistry, 2014, 38(11): 5260-5263.

[14] E. Spain, A. Mccooey, C. Dolan, H. Bagshaw, N. Leddy, R.J. Forster et al. Analyst. Electrodeposited gold-copper core-shell nanowires for high sensitivity

DNA detection. Analyst, 2014, 139(21):5504-8.

[15] N. Shahabadi, M. Maghsudi, S. Kashanian. A fluorescent sensor based on methyldopa drug modified γ-Fe_2O_3 nanoparticles for ultrasensitive detection of calf thymus DNA. Spectrochimica Acta Part A: Molecular and Biomolecular Spectroscopy, 2016, 157: 104-109.

[16] M. Trévisan, M. Schawaller, G. Quapil, E. Souteyrand, Y. Mérieux, J.P. Cloarec. Evanescent wave fluorescence biosensor combined with DNA bio-barcode assay for platelet genotyping. Biosensors and Bioelectronics, 2010, 26(26): 1631-1637.

[17] Z. Zhou, T. Li, H. Huang, Y. Chen, F. Liu, C. Huang, et al. A dual amplification strategy for DNA detection combining bio-barcode assay and metal-enhanced fluorescence modality. Chemical Communications, 2014, 50(87): 13373-13376.

[18] Y. Huang, S. Zhao, Y. Liu, J. Chen, Z. Chen, M Shi, et al. An amplified single-walled carbon nanotube-mediated chemiluminescence turn-on sensing platform for ultrasensitive DNA detection. Chemical Communications, 2012, 48(75): 9400-9402.

[19] Z. Xing, L. Wang, X Sun, Y.He, A.M. Asiri.Nanoporous molybdenum carbide nanowires: a novel sensing platform for DNA detection. Journal of Materials Chemistry B, 2015, 3(36): 7173-7176.

[20] W.R.G. Baeyens, S.G. Schulman, A.C. Calokerinos, Y. Zhao, K. Nakashima, D.DeKeukeleire, et al. Chemiluminescence-based detection: principles and analytical applications in flowing streams and in immunoassays. Journal of Pharmaceutical and Biomedical Analysis, 1998, 17(6-7): 941-53.

[21] A. Jain, A. Kumar, S.J. Dhoble, D.R. Peshwe. Persistent luminescence: An insight. Renewable and Sustainable Energy Reviews, 2016, 65: 135-153.

[22] A. Khataee, R. Lotfi, A. Hasanzadeh, M. Iranifam, S. W. Joo. Flow-injection chemiluminescence analysis for sensitive determination of atenolol using cadmium sulfide quantum dots. Spectrochimica Acta Part A: Molecular and Biomolecular Spectroscopy, 2016, 157: 88-95.

[23] H. Duan, L. Li, X. Wang, Y. Wang, J. Li, C. Luo. CdTe quantum dots@luminol as signal amplification system for chrysoidine with chemiluminescence-chitosan/graphene oxide-magnetite-molecularly imprinting sensor. Spectrochimica Acta Part A: Molecular and Biomolecular Spectroscopy, 2016, 153: 535-541.

[24] M. Iranifam. Chemiluminescence reactions enhanced by silver nanoparticles and silver alloy nanoparticles: Applications in analytical chemistry. Trac Trends in Analytical Chemistry, 2016, 82: 126-142.

[25] J. Wang, G. Zhao, L. Jing, X. Peng, Y. Li. Facile selfassembly of magnetite nanoparticles on three-dimensional graphene oxide-chitosan composite for lipase immobilization. Biochemical Engineering Journal, 2015, 98: 75-83.

[26] Z. Liu, A. Zhang, Y. Guo, C. Dong. Electrochemical sensor for ultrasensitive determination of isoquercitrin and baicalin based on DM-β-cyclodextrin functionalized graphenenanosheets. Biosensors and Bioelectronics, 2014, 58: 242-248.

[27] M. Khan, M. N Tahir, S.F .Adil, H.U. Khan, M.R.H. Siddiqu, W. Tremel, et al.

Graphene based metal and metal oxide nanocomposites synthesis, properties and their applications. Journal of Materials Chemistry A, 2015, 3(37): 18753-18808.

[28] B. Jiang, Q. Wu, N. Deng, Y. Chen, L. Zhang, L. Liang, et al. Hydrophilic GO/Fe_3O_4/Au/PEG nanocomposites for highly selective enrichment of glycopeptides. Nanoscale, 2016, 8(9): 4894-4897.

[29] H. Duan, X. Wang, Y. Wang, Y. Sun, J. Li, C. Luo. An ultrasensitive lysozyme chemiluminescence biosensor based on surface molecular imprinting using ionic liquid modified magnetic graphene oxide/b-cyclodextrin as supporting material. Analytica Chimica Acta, 2016, 918: 89-96.

[30] B. Korzeniowska, R. Nooney, D. Wencel and C. McDonagh. Silica nanoparticles for cell imaging and intracellular sensing. Nanotechnology, 2013, 24.

[31] Y. Wang, M. Zhang, L. Wang, W. Li, J. Zheng, J. Xu. Synthesis of hierarchical nickel anchored on Fe_3O_4@SiO_2 and its successful utilization to remove the abundant proteins (BHb) in bovine blood. New Journal of Chemistry, 2015, 39(6): 215-218.

[32] X. Chen, J. Zhu, Z. Chen, C. Xu, Y. Wang, C. Yao. A novel bienzyme glucose biosensor based on three-layer Au–Fe_3O_4@SiO_2 magnetic nanocomposite. Sensors and Actuators B: Chemical, 2011, 159(1): 220-228.

[33] X. Wu, Y. Shi, S. Zhong, H. Lin, J. Chen. Facile synthesis of Fe_3O_4-graphene @ mesoporous SiO_2 nanocomposites for efficient removal of Methylene Blue. Applied Surface Science, 2016, 378: 80-86.

[34] X. Liu, Y. Chen, C. Hao, J. Ye, R. Yu, D. Huang. Graphene-enhanced microwave

absorption properties of Fe_3O_4/SiO_2 nanorods. Composites: Part A, 2016, 89: 40-46.

[35] W. Wang, R. Ma, Q. Wu, C. Wang, Z. Wang. Magnetic microsphere-confined graphene for the extraction of polycyclic aromatic hydrocarbons from environmental water samples coupled with high performance liquid chromatography-fluorescence analysis. Journal of Chromatography A, 2013, 1293: 20-27.

[36] Y. Wang, Y. Lai, S. Wang, W. Jiang. Controlled synthesis and electromagnetic wave absorption properties of core-shell $Fe_3O_4@SiO_2$ nanospheres decorated grapheme. Ceramics International 2017, 43: 1887-1894.

[37] X. Sua, C. Chana, J. Shia, M. Tsangb, Y. Panc, et al. A graphene quantum dot@$Fe_3O_4@SiO_2$ based nanoprobe for drug delivery sensing and dual-modal fluorescence and MRI imaging in cancer cells.

[38] W.S. Hummers, R.E. Offeman, Preparation of graphitic oxide, Journal of the American Chemical Society, 1958, 80(6): 1339.

[39] R. Liu, R.D. Priestley. Rational design and fabrication of core–shell nanoparticles through a one-step/pot strategy. Journal of Materials Chemistry A, 2016, 4(18): 6680-6692.

[40] M.H. Nahm, L.A. Herzenberg, K. Little, J.R. Little. A new method of applying the Sips equation. The Journal of Immunology, 1977, 119 (1): 301-315.

[41] R. Sips. Combined form of Langmuir and Freundlich equations. The Journal of Chemical Physics, 1948, 16: 490-495.

[42] C. Zhang, H. Wang, C. Gao, E. Chen, H. Wang, et al. Equilibrium and kinetics studies of Cu (II) ions adsorption on polyamidoamine dendrimer starch. Research on Chemical Intermediates, 2012, 38:2411-2425.

[43] M. Abbas, S. Kaddour, M. Trari. Kinetic and equilibrium studies of cobalt adsorption on apricot stone activated carbon. Journal of Industrial and Engineering Chemistry, 2014, 20:745-751.

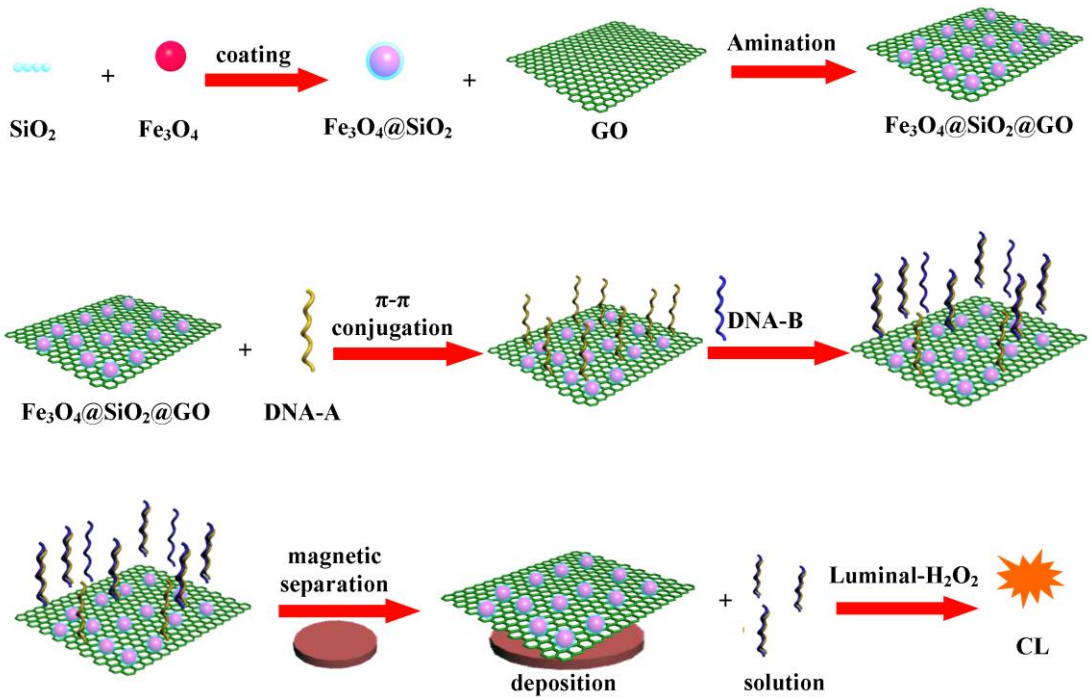

Graphical abstract

Highlight

1. A CL biosensor for DNA was obtained based on Fe_3O_4@SiO_2@GO.

2. The complementary base pairing of DNA improved selectivity of the biosensor.

3. Adsorption of Fe_3O_4@SiO_2@GO to DNA followed Langmuir isotherm.

4. Adsorption of Fe_3O_4@SiO_2@GO to DNA followed pseudo-second order sorption kinetics.